Bismuth Borates: One-Dimensional Borate Chains and Nonlinear Optical Properties

Linyan Li, Guobao Li, Yingxia Wang, Fuhui Liao, and Jianhua Lin*

State Key Laboratory of Rare Earth Materials Chemistry and Applications, College of Chemistry and Molecular Engineering, Peking University, Beijing 100871, P. R. China

Three bismuth borates, $Bi[B_4O_6(OH)_2]OH$ (**I**), BiB_2O_4F (**II**), and $Bi_3[B_6O_{13}(OH)]$ (**III**), were obtained in boric acid flux at low temperatures and their structures were determined by using single-crystal and powder X-ray diffraction techniques. All these three bismuth borates contain one-dimensional borate chains and crystallize in noncentrosymmetric space groups. **I** is a hydrated borate, crystallizing in the space group $P1$ with lattice constants $a = 4.300(1)$ Å, $b = 8.587(2)$ Å, $c = 10.518(2)$ Å, $\alpha = 113.11(3)°$, $\beta = 100.50(3)°$, and $\gamma = 90.36(3)°$, and the borate chain consists of a 3-ring ($2BO_3 + BO_4$) and a BO_3 group. **II** is a fluoroborate, which crystallizes in the trigonal space group $P3_2$ with $a = 6.7147(1)$ Å and $c = 6.4688(1)$ Å, and the borate anion is a 3-fold helix chain formed by extensive linkage of three-membered borate rings ($3BO_4$). **III** is also a hydrated borate with a structure that is closely related to **II**, in which one-sixth of the borate groups are in triangular geometry (BO_3), which reduces the symmetry to $P1$, $a = 6.6257(1)$ Å, $b = 6.6238(1)$ Å, $c = 6.6541(1)$ Å, and $\alpha = 89.998(3)°$, $\beta = 89.982(2)°$, and $\gamma = 119.992(2)°$. All these three bismuth borates exhibit nonlinear optical (NLO) properties.

Introduction

Borate is a large resource for functional materials, particularly for nonlinear optical (NLO) materials. β-$Ba_2B_2O_4$ (BBO)[1] is a well-known example that exhibits promising NLO property. Recently, considerable interest was focused on α-BiB_3O_6 (BIBO) due to its largest second-harmonic (SHG) coefficients over other known NLO borates, such as $KTiOPO_4$ (KTP), BBO, LiB_3O_5 (LBO), or $LiIO_3$.[2−5] Besides α-BiB_3O_6,[6] the bismuth borates known so far include $Bi_4B_2O_9$,[7] $Bi_6B_{10}O_{24}$,[8] $Bi_2B_8O_{15}$,[9,10] and $Bi_{24.5}BO_{38.25}$[11] and all of them were synthesized by high-temperature solid-state reactions. Recently, we have been using extensively boric acid as a flux to study the formation of borates at relatively low temperatures.[12−14] By systematic study of the bismuth borate system, we identified a series of new bismuth borates

including $Bi[B_4O_6(OH)_2]OH$, BiB_2O_4F, $Bi_3[B_6O_{13}(OH)]$, β-BiB_3O_6, and γ-BiB_3O_6. These five bismuth borates can be classified into two groups. The first three compounds all contain one-dimensional borate chains and exhibit NLO properties, while β-BiB_3O_6 and γ-BiB_3O_6 are the two new polymorphs of BiB_3O_6 crystallizing in the structures closely related to α-BiB_3O_6. Herein this paper we report the syntheses, structures, and NLO properties of the one-dimensional borate compounds. The other two compounds, i.e., β-BiB_3O_6 and γ-BiB_3O_6, will be discussed in a separate paper.[15]

Experimental Section

Synthesis. Syntheses of bismuth borates, $Bi[B_4O_6(OH)_2]OH$ (**I**), BiB_2O_4F (**II**), and $Bi_3[B_6O_{13}(OH)]$ (**III**), were carried out in closed Teflon autoclaves using boric acid as a flux. The starting materials, H_3BO_3, $Bi(NO_3)_3 \cdot 5H_2O$ or Bi_2O_3 and NaF, used in the syntheses are all analytical grade. The obtained products depend strongly on reaction conditions, i.e., the ratio of the starting materials and the reaction temperatures. $Bi[B_4O_6(OH)_2]OH$ (**I**) was synthesized by using H_3BO_3 (3.09 g) and $Bi(NO_3)_3 \cdot 5H_2O$ (1.21 g) as the starting materials and the reaction was proceeded in a 50 mL Teflon autoclave at 200 °C for 7 days. BiB_2O_4F (**II**) was obtained by using NaF as a fluorine source. In practice, 3.09 g of H_3BO_3, 1.21 g of $Bi(NO_3)_3 \cdot 5H_2O$, and 0.2 g of NaF were mixed and the reaction was carried out in a 50 mL Teflon autoclave at 240 °C for 7 days. For $Bi_3[B_6O_{13}(OH)]$ (**III**), 3.09 g of H_3BO_3, 0.58 g of Bi_2O_3, and

* To whom correspondence should be addressed. E-mail: jhlin@pku.edu.cn. Tel: (8610)62751715. Fax: (8610)62751708.

(1) Chen, C. T.; Wu, B. C.; Jiang, A. D.; You, G. M. *Sci. Sinica (China)* **1985**, *B28*, 235.

(2) Hellwig, H.; Liebertz, J.; Bohatý, L. *Solid State Commun.* **1999**, *109* (4), 249.

(3) Hellwig, H.; Liebertz, J.; Bohatý, L. *J. Appl. Phys.* **2000**, *88* (1), 240.

(4) Lin, Z. S.; Wang, Z. Z.; Chen, C. T.; Lee, M. H. *J. Appl. Phys.* **2001**, *90* (11), 5585.

(5) Wang, J. Y.; Wang, Z. P.; Jiang, H. D.; Hu, X. B.; Song, R. B.; Liu, H.; Liu, Y. G.; Wei, J. H.; Shao, Z. S. *J. Cryst. Growth* **2001**, *224*, 280.

(6) Fröhlich, R.; Bohat×c6, L.; Liebertz, J. *Acta Crystallogr.* **1984**, *C40*, 343.

(7) Hyman, A.; Perloff, A. *Acta Crystallogr.* **1972**, *B28*, 2007.

(8) Vegas, A.; Cano, F. H.; García-Blanco, S. *J. Solid State Chem.* **1976**, *17*, 151.

(9) Teng, B.; Yu, W. T.; Wang, J. Y.; Cheng, X. F.; Dong, S. M.; Liu, Y. G. *Acta Crystallogr.* **2002**, *C58*, i25.

(10) Egorysheva, A. V.; Kanishcheva, A. S.; Kargin, Yu. F.; Gorbunova, Yu. E.; Mikhailov, Yu. N. *Russ. J. Inorg. Chem.* **2002**, *47* (12), 1804.

(11) Burianek, M.; Held, P.; Mühlberg, M. *Cryst. Res. Technol.* **2002**, *37*, 785.

(12) Lu, P. C.; Wang, Y. X.; Lin, J. H.; You, L. P. *Chem. Commun.* **2001**, 1178.

(13) Li, L. Y.; Lu, P. C.; Wang, Y. Y.; Jin, X. L.; Li, G. B.; Wang, Y. X.; You, L. P.; Lin, J. H. *Chem. Mater.* **2002**, *14*, 4963.

(14) Li, L. Y.; Jin, X. L.; Li, G. B.; Wang, Y. X.; Liao, F. H.; Yao, G. Q.; Lin, J. H. *Chem. Mater.* **2003**, *15*, 2253.

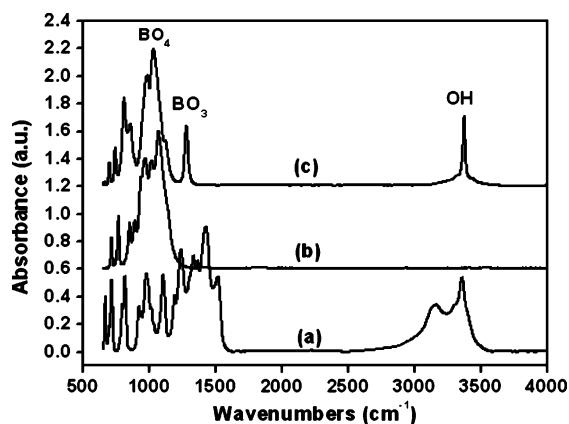(15) Li, L. Y.; Li, G. B.; Wang, Y. X.; Liao, F. H.; Lin, J. H., in preparation.

Figure 1. IR spectrum of $Bi[B_4O_6(OH)_2]OH$ (a), $BiBiB_2O_4F$ (b), and $Bi_3[B_6O_{13}(OH)]$ (c).

5 mL of H_2O were charged in a 25 mL Teflon autoclave and the reaction was proceeded at 200 °C for 7 days. The products obtained from reactions were mixtures containing corresponding bismuth borates and excess boric acid and, for the fluoroborate case (**II**), excess sodium fluoride. The boric acid and sodium fluoride can be removed by washing the products with hot water (yield: 90% for **I** and **II**; 85% for **III** based on Bi, respectively).

Characterizations. Chemical analyses for bismuth and boron were performed with inductively coupled plasma (ICP) and the measured B:Bi mole ratios are 4.11 for **I**, 1.93 for **II**, and 2.06 for **III**, respectively. X-ray fluorescence measurement on **II** revealed that the Bi:F mole ratio is about 1:1. TGA measurements, carried out on a Dupont 1090 instrument, were used to track the weight loss of hydroxyl groups at high temperature. IR spectra recorded on a Nickel Magna-750 FT-IR spectrometer were used as independent evidence for the geometry of borate groups and the presence of hydroxyl groups in the compounds. In Figure 1, we show the IR spectra of these three bismuth borates, which clearly indicate the presence of BO_3, BO_4, and OH in **I** and **III**. In contrast, **II** contains only tetrahedral borate BO_4 and no detectable hydroxyl group was observed. The second-harmonic generation (SHG) coefficients were measured by the Kurtz-Perry method on powder samples.[16] The incident light is 1064 nm from a YAG:Nd^{3+} laser and the frequency-doubled outputs ($\lambda = 532$ nm) were recorded by using KDP as a reference.

Structure Determinations

$Bi[B_4O_6(OH)_2]OH$ (I). A colorless crystal **I** of approximate dimensions $0.2 \times 0.1 \times 0.05$ mm^3 was selected and mounted on a BRUKER SMART X-ray diffractometer with an APEX-CCD area detector using graphite monochromated Mo Kα radiation ($\lambda = 0.71073$ Å) at 50 kV and 30 mA at room temperature. A total of 3304 reflections were collected in the range $4.30° \leq 2\theta \leq 66.98°$, of which 2886 were independent and 2702 were observed ($I > 2\sigma$). The structure **I** crystallizes in the space group $P1$. An empirical absorption correction was applied based on symmetry-equivalent reflections using the SADABS program[17] (2486 unique reflections, $R_{int} = 0.0291$). The crystal structure was solved by using direct methods (SHELXS97)[18] and subsequent different Fourier analyses. The final refinements were carried out by full-matrix least-squares on F^2 using all unique

data with SHELXL97[18] with the isotropic displacement parameters, R1 = 0.0375 and wR2 = 0.1009. The hydrogen atoms were incorporated to the oxygen based on bond valance sum calculation. The crystallographic data are given in Table 1. The atomic coordinates with isotropic temperature factor are listed in Table 2 and selected bond lengths are listed in Table 3.

BiB_2O_4F (II). The crystals of **II** were too small for single-crystal study. Therefore, the structure was solved by the powder X-ray diffraction technique. Powder X-ray diffraction data were collected on a Bruker D8 Advance diffractometer with Cu Kα_1 ($\lambda = 1.54056$ Å) radiation (2θ range: 12−120°; step: 0.02°; scan speed: 60 s/step) at 50 kV and 40 mA at room temperature. The powder diffraction data can be readily indexed to a hexagonal cell.[19] The systematic absence of the reflections indicated a trigonal space group, $P3_1$ or $P3_2$. The bismuth and part of oxygen atoms were located directly from the direct method[20] and subsequent different Fourier analysis[21] was used for locating the rest of the oxygen and boron positions. The structure was refined using the Rietveld method[22] with isotropic displacement parameters. Considering the small scattering factor of boron atoms, soft constraint of B−O distances were applied during the refinement; otherwise, a few B−O distances showed large deviation from the ideal value. To testify the possible oxygen vacancy in the structure, the occupation factors of the oxygen atoms were refined. The refined occupation factors are close to unit (0.96−1.10), indicating that no significant oxygen vacancies are present in this compound. In Figure 2a we show the profile fitting of the final refinement. The crystallographic data are given in Table 1, and the atomic parameters and selected bond distances are listed in Table 4 and Table 5.

$Bi_3[B_6O_{13}(OH)]$ (III). The X-ray powder diffraction pattern of **III** is very similar to **II**. Initially, we indexed the XRD pattern[19] with a similar hexagonal cell, $a = 6.625$ and $c = 6.654$ Å, and attempted to refine the structure with the structure model **II**. At this stage, it was clear that only the bismuth position and part of the borate chain can be defined within the trigonal symmetry. Remarkable mismatching of certain reflections yielded a large residue value Rwp = 0.23, indicating that the symmetry of the structure should be lower. When the trigonal cell is retained, but the 3-fold axis is removed from $P3_2$, the only possible space group for the structure **III** is $P1$. The lower symmetry of the structure **III** is also evidenced by the presence of the small portion of BO_3 groups in the compound as indicated by the IR spectrum (Figure 1c). To build the triclinic model, we first identified the bismuth and part of the borate chain by symmetry

(16) Kurtz, S. K.; Perry, T. T. *J. Appl. Phys.* **1968**, *39*, 3798.
(17) Sheldrick, G. M. *SADABS, Siemens Area Detector Absorption Correction Program*; University of Göttingen: Göttingen, 1994.
(18) Sheldrick, G. M. *SHELXS 97, Program for the solution of crystal structures*; University of Göttingen: Göttingen, 1997. *SHELXL 97, Program for the refinement of crystal structures*; University of Göttingen: Göttingen, 1997.
(19) Dong, C. *J. Appl. Crystallogr.* **1999**, *32*, 838.
(20) Altomare, A.; Burla, M. C.; Cascarano, G.; Giacovazzo, C.; Guagliardi, A.; Moliterni, A. G. G.; Polidiori, G. *J. Appl. Crystallogr.* **1995**, *28*, 842.
(21) Altomare, A.; Cascarana, G.; Giacovazzo, C.; Guagliardi, A. *SIRPOW user's manual*; Inst. Di Ric. Per lo Sviluppo di Metodologie Cristallografiche, CNR.
(22) Larson, A. C.; von Dreele, R. B. Report LAUR 86-748; Los Alamos National Laboratory: Los Alamos, NM, 1985.

Table 1. Crystal Data and the Structure Refinement of Bi[B₄O₆(OH)₂]OH (I), BiB₂O₄F (II) and Bi₃[B₆O₁₃((OH)] (III)

formula	Bi[B$_4$O$_6$(OH)$_2$]OH	BiB$_2$O$_4$F	Bi$_3$[B$_6$O$_{13}$(OH)]
formula mass	399.22	313.60	916.79
crystal system	triclinic	trigonal	triclinic
space group	$P1$	$P3_2$	$P1$
a/Å	4.300(1)	6.7147(1)	6.6257(1)
b/Å	8.587(2)		6.6238(1)
c/Å	10.518(2)	6.4688(1)	6.6541(1)
α/°	113.11(3)	90	89.998(3)
β/°	100.50(3)	90	89.982(2)
γ/°	90.36(3)	120	119.992(2)
V/Å^3	349.90(15)	252.225 (3)	252.923(8)
Z	2	3	1
density (calc.) (g/cm^3)	3.761	6.196	6.021
reflections	3304 (2886 > 2σ)	254 reflections	250 reflections
λ/Å	0.71073		1.5405
μ(Mo Kα)/mm^{-1}	25.18		
diffraction techniques	single crystal	powder diffraction	
structure determination	direct method	direct method, expo	
structure refinement	SHELX98	GSAS and TOPAS with pseudovoigt peak function	
largest diff. peak/hole/e·Å^{-3}	4.47/−4.53		
GOF	0.982	1.224	1.747
final R indices	R1 = 0.0375	R_p = 0.104	R_p = 0.0654
	wR2 = 0.1009	R_{wp} = 0.148	R_{wp} = 0.0893

Table 2. Fractional Atomic Coordinates and Isotropic Thermal Displacement Parameters for Bi[B₄O₆(OH)₂]OH (I)[a]

atom	x	y	z	U(eq)	BVS
Bi1	0.95118(5)	0.51273(4)	0.90012(4)	0.0098(2)	3.04
Bi2	0.24814(7)	0.15961(5)	0.98078(4)	0.0118(2)	3.10
O1	0.995(4)	0.104(2)	0.184(2)	0.013(3)	1.87
O2	0.194(4)	0.567(2)	0.696(2)	0.013(3)	2.16
O3	0.112(4)	0.935(2)	0.320 (1)	0.013(3)	1.90
O4	0.869(4)	0.798(2)	0.077(1)	0.018(3)	2.01
O5	0.419(3)	−0.076(2)	0.149(2)	0.012(3)	1.66
O6	0.839(4)	0.188(2)	0.406(1)	0.011(3)	1.76
OH7	0.521(5)	0.344(2)	0.619(2)	0.017(3)	0.92
OH8	0.679(4)	0.331(3)	0.254(2)	0.017(3)	1.12
O9	0.094(5)	0.737(2)	0.556(2)	0.022(4)	1.80
O10	0.340(5)	0.484(3)	0.471(2)	0.021(4)	1.94
O11	0.325(3)	0.874(2)	0.804(2)	0.015(3)	2.05
O12	0.806(4)	0.755(2)	0.737(2)	0.014(3)	2.12
OH13	0.956(5)	0.032(3)	0.552(2)	0.030(4)	0.85
OH14	0.230(5)	0.634(2)	0.337(2)	0.020(3)	1.18
O15	0.412(4)	0.619(2)	0.999(2)	0.018(3)	2.24
O16	0.775(3)	0.051(2)	0.881(2)	0.014(3)	1.88
OH17	0.979(4)	0.397(2)	0.055(1)	0.013(3)	1.33
OH18	0.212(4)	0.271(2)	0.831(2)	0.021(4)	1.50
B1	0.973(8)	0.036(4)	0.424(2)	0.017(5)	2.82
B2	0.092(6)	−0.056(4)	0.184(2)	0.019(6)	3.05
B3	0.845(6)	0.218(3)	0.290(2)	0.012(4)	3.00
B4	0.098(5)	0.734(2)	0.698(2)	0.009(4)	3.17
B5	0.358(6)	0.478(3)	0.606(2)	0.009(4)	3.02
B6	0.209(8)	0.618(3)	0.454(3)	0.014(5)	3.38
B7	0.654(4)	0.872(2)	0.821(2)	0.005(3)	2.88
B8	0.556(4)	0.777(2)	0.084(2)	0.003(2)	2.98
H7	0.66(7)	0.32(3)	0.57(3)	0.026^a	
H8	0.59(7)	0.39(4)	0.32(3)	0.025^a	
H13	0.96(7)	0.93(4)	0.54(3)	0.045^a	
H14	0.05(5)	0.63(3)	0.29(2)	0.030^a	
H17	0.89(10)	0.44(6)	0.14(4)	0.019^a	
H18	0.29(12)	0.23(6)	0.75(5)	0.031^a	

[a] H atoms were located from the difference electrons density map. The positional parameters of the H atoms were calculated by fixed H−O distances (0.82 Å for O7, O8, O13, and O14; 0.93 Å for O17 and O18). The U_{eq}(H) were fixed to a value that is 1.5 times that of the U_{eq}(O) of the parent atoms.

transformation ($P3_2 \rightarrow P1$). The complete borate framework was established by using a simulated annealing technique (Topas[23]) in which the rigid tetrahedral and triangular borate groups were used as the building blocks. Then the structure

(23) *User's Manual of Topas-R*; Bruker GmbH: Karlsruhe, Germany, 2003.

Table 3. Selected Bond Distances (Å) for Bi[B₄O₆(OH)₂]OH (I)

	bond distance (Å)		bond distance (Å)
Bi1−O15	2.078(18)	Bi2−O18	2.124(17)
Bi1−O17	2.202(10)	Bi2−O16	2.130(12)
Bi1−O18	2.286(17)	Bi2−O17	2.282(15)
Bi1−O4	2.499(16)	Bi2−O11	2.499(16)
Bi1−O15	2.729(16)	Bi2−O16	2.689(17)
Bi1−O2	2.745(15)	Bi2−O1	2.759(14)
B1−O3	1.34(3)	B5−O2	1.29(3)
B1−O6	1.49(4)	B5−O7	1.40(3)
B1−O13	1.37(3)	B5−O10	1.43(2)
B2−O1	1.43(3)	B6−O9	1.33(3)
B2−O3	1.45(2)	B6−O10	1.34(3)
B2−O4	1.50(3)	B6−O14	1.31(3)
B2−O5	1.51(3)	B7−O11	1.39(2)
B3−O1	1.43(2)	B7−O12	1.32(3)
B3−O6	1.36(2)	B7−O16	1.46(2)
B3−O8	1.33(3)	B8−O4	1.38(2)
B4−O2	1.48(3)	B8−O5	1.38(2)
B4−O9	1.51(3)	B8−O15	1.36(2)
B4−O11	1.47(2)		
B4−O12	1.38(3)		

	Averaged B−O Distances		
B1−O	1.40	B5−O	1.37
B2−O	1.47	B6−O	1.33
B3−O	1.37	B7−O	1.39
B4−O	1.46	B8−O	1.37

was refined using the Rietveld method. The refined lattice constants are very close to the hexagonal cell. The structure refinement was conducted with great caution because of the strong overlap of the nonequivalent reflections. In the final stage of the refinement, the unrealistic B−O bond distances were adjusted by partial refinement with bond-length restraint. The structure study yields a composition Bi$_3$B$_6$O$_{14}$ for **III** and, considering the charge balance, the formula should be Bi$_3$[B$_6$O$_{13}$(OH)]. From a crystallographic point of view, the triclinic structure of **III** may only be considered as a tentative structure model. More accurate structure determination may need single-crystal data for this low-symmetry structure. Figure 2b shows the profile fitting of the diffraction pattern. The crystallographic data are given in Table 1, and the atomic parameters and bond distances are listed in Table 6 and Table 7.
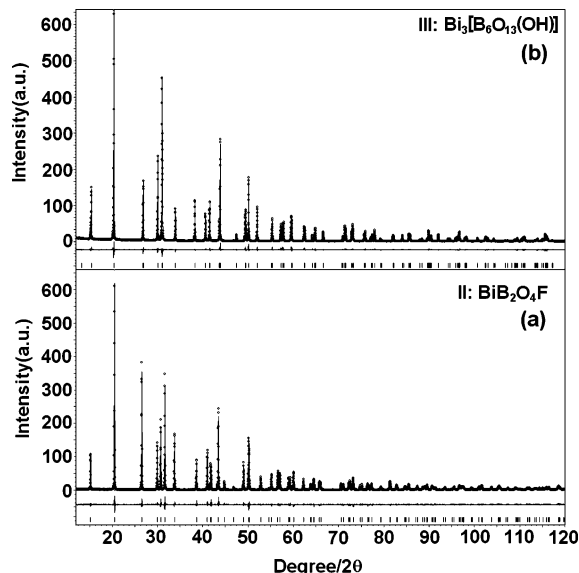
Figure 2. Profile fit to the powder X-ray diffraction pattern of BiB_2O_4F (a) and $Bi_3[B_6O_{13}(OH)]$ (b). The symbol + represents the observed value and solid line represents the calculated value; the marks below the diffraction patterns are the calculated reflection positions and the difference curve is shown at the bottom of the figure.

Table 4. Fractional Atomic Coordinates and Isotropic Thermal Displacement Parameters for BiB_2O_4F (II)[a]

atom	x	y	z	BVS
Bi1	0.7069(3)	0.9400(4)	0.4524(24)	2.90
O1	0.574(5)	0.295(6)	0.898(4)	2.10
O2	0.853(6)	0.666(5)	0.530(4)	1.83
O3	0.977(5)	0.534(4)	0.808(4)	2.17
O4(F)	0.232(8)	0.766(7)	0.544(4)	1.14(O^{2-})
				0.96(F^-)
O5	0.104(4)	0.902(4)	0.795(4)	2.20
B1	0.551(10)	0.235(10)	0.117(13)	3.34
B2	0.041(10)	0.719(6)	0.665(5)	3.49

[a] The displacement parameters were constrained for the same elements ($U_{eq}(Bi1) = 0.0073$, $U_{eq}(O) = 0.0097$, and $U_{eq}(B) = 0.0237$).

Table 5. Selected Bond Distances (Å) for BiB_2O_4F (II)

bond distance (Å)		bond distance (Å)	
Bi1−O5	2.241(24)	B1−O1	1.42(7)
Bi1−O5	2.321(21)	B1−O1	1.46(10)
Bi1−O1	2.397(23)	B1−O2	1.42(8)
Bi1−O3	2.436(25)	B1−O3	1.45(6)
Bi1−O2	2.528(25)	B2−O2	1.43(6)
Bi1−O4(F)	2.850(40)	B2−O3	1.43(4)
Bi1−O3	2.896(30)	B2−O4(F)	1.40(6)
Bi1−O2	2.921(28)	B2−O5	1.37(4)
Bi1−O4(F)	2.985(27)		

Averaged B−O Distances			
B1−O	1.44	B2−O	1.41

Results and Discussion

Formation of Bismuth Borates. Boric acid melts at about 175 °C and thus can be used as a flux at low temperature in a closed system. In practice, however, the ratio of starting materials and reaction temperatures may influence the products. **I** is a hydrated borate and can be obtained by direct reaction of bismuth nitrate with boric acid at 200 °C. However, a small amount of water ($H_2O:B_2O_3$ is about 1:1) in the reaction system can significantly improve the crystallinity and phase purity of **I**. The fluoroborate **II** was obtained in boric acid flux at 240 °C in the presence of NaF. Without

Table 6. Fractional Atomic Coordinates for $Bi_3[B_6O_{13}((OH)]$ (III)[a]

atom	x	y	z	atom	x	y	z
Bi11	0.9196	0.64747	0.4587	O21	0.998	0.479	0.096
Bi12	0.3021	0.13256	0.7994	O22	0.508	0.444	0.384
Bi13	0.8013	0.02529	0.138	O23	0.552	0.955	0.768
B11	0.957	0.635	0.976	O31	0.878	0.231	0.549
B12	0.764	0.010	0.655	O32	0.434	0.095	0.198
B13	0.325	0.204	0.313	O41	0.138	0.743	0.837
B21	0.354	0.729	0.826	O42	0.714	0.835	0.507
B22	0.232	0.534	0.166	O43	0.222	0.311	0.199
B23	0.484	0.627	0.484	O51	0.317	0.671	0.363
O11	0.758	0.648	0.005	O52	0.361	0.554	0.684
O12	0.914	0.015	0.817	O53	0.411	0.675	0.012
O13	0.185	0.048	0.476				

[a] The structure of **III** was refined with a rigid body constraint for borate groups; therefore, the deviations of the atomic positions are not listed for oxygen and boron. The displacement parameters were refined for bismuth atoms ($U_{eq}(Bi1) = 0.014(2)$, $U_{eq}(Bi2) = 0.011(2)$, and $U_{eq}(Bi3) = 0.011(2)$ but fixed for oxygen and boron $U_{eq}(O) = 0.01$ and $U_{eq}(B) = 0.01$). The atoms are labeled topologically related to **II**; for example, O11, O12, and O13 are topologically related to O1 in **II**.

Table 7. Selected Bond Distances (Å) for $Bi_3[B_6O_{13}((OH)]$ (III)

bond distance (Å)		bond distance (Å)		bond distance (Å)	
Bi11−O42	2.281	Bi12−O41	2.256	Bi13−O12	2.276
Bi11−O13	2.344	Bi12−O13	2.260	Bi13−O43	2.502
Bi11−O22	2.409	Bi12−O12	2.286	Bi13−O11	2.530
Bi11−O51	2.638	Bi12−O23	2.474	Bi13−O53	2.603
Bi11−O31	2.697	Bi12−O52	2.725	Bi13−O21	2.626
Bi11−O21	2.816	Bi12−O32	2.845	Bi13−O42	2.687
Bi11−O41	2.818			Bi13−O32	2.722
				Bi13−O23	2.869
B11−O11	1.37	B12−O42	1.43	B13−O43	1.42
B11−O41	1.39	B12−O31	1.45	B13−O13	1.47
B11−O21	1.44	B12−O12	1.45	B13−O32	1.47
		B12−O23	1.47	B13−O22	1.51
B21−O53	1.40	B22−O43	1.47	B23−O22	1.47
B21−O23	1.47	B22−O21	1.48	B23−O42	1.47
B21−O41	1.48	B22−O53	1.48	B23−O52	1.51
B21−O52	1.51	B22−O51	1.53	B23−O51	1.51

Averaged B−O Distances					
B11−O	1.40	B12−O	1.45	B13−O	1.47
B21−O	1.47	B22−O	1.49	B23−O	1.49

NaF, instead of **II** one obtained γ-BiB_3O_6.[15] **III** is also a hydrated bismuth borate and is formed only in the presence of a certain amount of water (mole ratio is about $B:Bi:H_2O = 20:1:100$) at 200 °C. Without water, **I** would appear as a primary phase. With a large amount of water (hydrothermal condition), a known bismuth borate $Bi_6B_{10}O_{24}$ was formed.

Thermal Stability. Thermal gravity analysis shows that all three compounds, **I**, **II**, and **III**, lose weight in certain temperature ranges. **I** is a hydrated bismuth borate, $Bi[B_4O_6(OH)_2]OH$; it loses about 6.1 wt % weight between 400 °C and 550 °C due to the dehydration of the hydroxyl groups. The decomposition product is a known bismuth borate, $Bi_2B_8O_{15}$[9,10] (calculated weight loss: 6.76 wt %). Compound **II** retained up to 450 °C in air and then gradually losses the weight up to 700 °C, resulting in a known bismuth borate, $Bi_6B_{10}O_{24}$ (exp. 6.0 wt %). **II** is a fluoroborate and the decomposition originates from the volatile BF_3 (calcd. 7.2 wt %). The hydrated borate **III** is less stable and started to lose weight at about 290 °C. The total weight loss was about 2.5 wt % up to 450 °C. The XRD measurement on a sample of **III** annealed at 650 °C indicated that the decomposition product is $Bi_6B_{10}O_{24}$. According to the

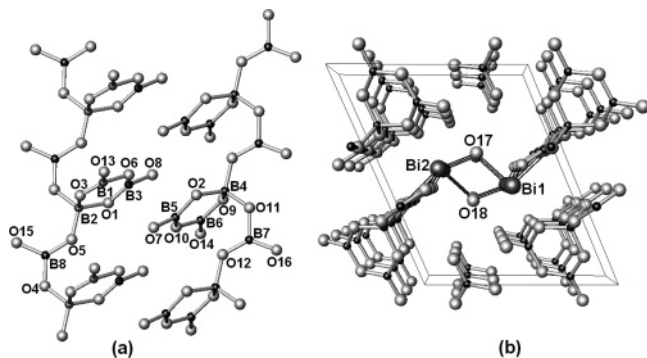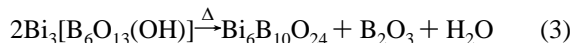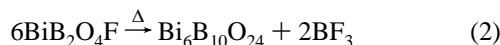**Figure 3.** The one-dimensional borate chain of Bi[B$_4$O$_6$(OH)$_2$]OH (a), between which the bismuth ions and the hydroxyl groups are located (b).

Figure 4. (a) The perspective view of the structure of BiB$_2$O$_4$F along the *c*-axis; (b) the helical borate chain of BiB$_2$O$_4$F.

decomposition reaction (eq 3), the expected weight loss is about 1.0 wt % if only water is taken into account.

$$2Bi[B_4O_6(OH)_2]OH \xrightarrow{\Delta} Bi_2B_8O_{15} + 3H_2O \qquad (1)$$

$$6BiB_2O_4F \xrightarrow{\Delta} Bi_6B_{10}O_{24} + 2BF_3 \qquad (2)$$

$$2Bi_3[B_6O_{13}(OH)] \xrightarrow{\Delta} Bi_6B_{10}O_{24} + B_2O_3 + H_2O \qquad (3)$$

Structure of Bi[B$_4$O$_6$(OH)$_2$]OH (I). Bi[B$_4$O$_6$(OH)$_2$]OH crystallizes in a triclinic structure that contains 28 crystallographic independent atoms (2Bi, 18O, and 8B). The borate anions in the structure are one-dimensional chains parallel to the *a*-axis. As shown in Figure 3a, a BO$_3$ and a BO$_4$ share a corner forming the backbone of the borate chains. The other two oxygen atoms on the BO$_4$ further connect to a B$_2$O$_5$ group forming the side 3-ring (2BO$_3$ + BO$_4$). The fundamental building block of the borate chain is a B$_4$O$_9$ unit consisting of a 3-ring (2BO$_3$ + BO$_4$) and a BO$_3$ group. As far as the charge balance is concerned, there are three hydrogen atoms per formula Bi[B$_4$O$_6$(OH)$_2$]OH. Based on bond valence sums (BVS) calculations[24] (Table 2), the hydrogen atoms should locate on the terminal oxygen atoms of 3-rings (O8, O13, O7, O14). The other two hydrogen atoms may most likely locate at the isolated oxygen atoms (BVS is 1.33 for O17 and 1.5 for O18). These two hydroxyl groups coordinate to Bi ions forming a quadrangular cluster (Bi$_2$O$_2$) as shown in Figure 3b. The other two terminal oxygen atoms (O15, O16) on the BO$_3$ groups of the backbone are deprotonated with strong Bi–O bonds (Bi1–O15: 2.078 and Bi1–O16: 2.130 Å). The coordination polyhedron of bismuth is irregular with the Bi–O bond length ranging from 2.078 to 2.759 Å (Table 3). Such irregular coordination is common for bismuth borates[6–10] due to the lone electron pair. If only those oxygen atoms with Bi–O distances less than 2.6 Å are taken into account, the coordination polyhedron of bismuth atom is a trigonal bipyramid when an electron lone pair is included as a ligand.

Structure of BiB$_2$O$_4$F (II). II is a fluoroborate containing 8 crystallographic sites, i.e., 1Bi, 5O (or 4O, 1F), and 2B (Table 4). The borate anion in the structure forms infinite helical chains that coordinate to the bismuth cations. In Figure 4a, we show a perspective view of the structure along
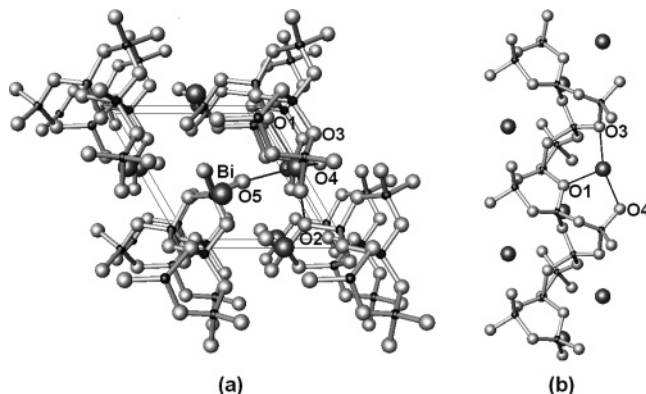
the *c*-axis. One of these borate helices are emphasized in Figure 4b. One can see that the 3-ring [B$_3$O$_8$F] unit can be considered as a fundamental building block (FBB), which shares two boron atoms forming a one-dimensional chain. There are two groups of oxygen atoms; O1, O2, and O3 are bridged to two boron atoms and O4(F) and O5 are terminal oxygen atoms. The bismuth cations are located within the cavities of the borate helices. In such a sense, the structure of **II** could be regarded as a helix of borate chain that catches metal cations. The bismuth atoms are bonded by O1, O3, and O4(F) within the chain and O2 and O5 crossing the chains.

As indicated, all of the atomic positions in **II** were well-defined in the structure refinement. However, as far as the charge balance is concerned, one-fifth of the oxygen positions should be occupied by fluorine. The structure refinement cannot differentiate oxygen and fluorine. However, the bond valance sums calculation (Table 4) indicates the oxidation state of the O4 site is significantly lower (BVS = −1.14 with O^{2-} and −0.96 with F$^-$) than the rest of oxygen (from −1.83 for O2 to −2.20 for O5). This suggests that the fluorine atoms are most likely located at the O4 position. In addition, many other evidences support the substitution of fluorine in the structure. First, this phase can only be formed in the presence of NaF in the reaction system. Second, the X-ray fluorescence measurement indicated unambiguously the presence of fluorine in this phase. Furthermore, the absence of OH groups and exclusively tetrahedral coordination of boron atoms in the structure as confirmed by the IR spectrum (Figure 1b) excludes the possibility of being a hydrated bismuth borate (BiB$_2$O$_4$(OH)). In fact, the fluoroborate ions are fairly common in solid-state compounds. RbBF$_4$, NH$_4$BF$_4$,[25] and BaBOF$_3$[26] were known to have B–F bonds in the fluoroborate ions. There are also some other solid-state compounds, such as Ln$_3$(BO$_3$)$_2$F$_3$[27] and Zn$_2$(BO$_3$)(OH)$_{0.75}$F$_{0.25}$,[28] which contain isolated fluorine anions. For BiB$_2$O$_4$F (**II**), all evidences mentioned above support it being a fluoroborate.

(24) Brese, N. E.; O'Keeffe, M. *Acta Crystallogr.* **1991**, *B 47*, 192.

(25) Hoard, J. L.; Blair, V. *J. Am. Chem. Soc.* **1935**, *57*, 1985.
(26) Chackraburtty, D. M. *Acta Crystallogr.* **1957**, *10*, 199.
(27) Corbel, G.; Retoux, R.; Leblanc, M. *J. Solid State Chem.* **1998**, *139*, 52.
(28) Corbel, G.; Suard, E.; Emery, J.; Leblanc, M. *J. Alloy Compd.* **2000**, *305*, 49.

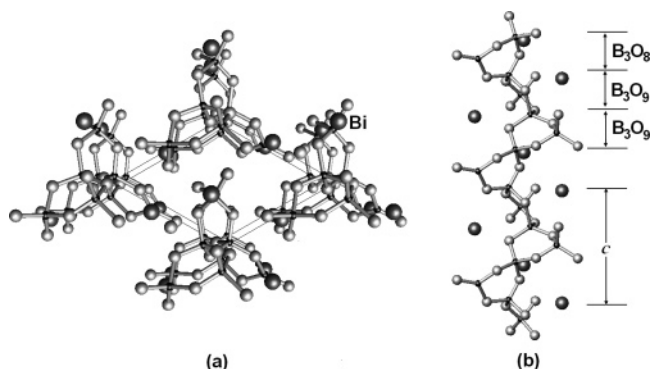**Figure 5.** (a) The perspective view of the structure of $Bi_3[B_6O_{13}(OH)]$ along the c-axis; (b) the helical borate chain of $Bi_3[B_6O_{13}(OH)]$.

Figure 6. The helical borate chains in **II** (a), **III** (b), and $Pb_6B_{11}O_{18}(OH)_9$ (c).

Structure of $Bi_3[B_6O_{13}(OH)]$ (III). III is a hydrated bismuth borate and was obtained by direct reaction of boric acid and bismuth oxide in the presence of a certain amount of water. Similar to **II**, the structure of **III** consists of also a helical borate chain that is surrounded by bismuth cations. However, as shown in Figure 5, the helical chain in $Bi_3[B_6O_{13}(OH)]$ (**III**) contains two different 3-ring borate units, $[B_3O_9]$ and $[B_3O_8]$, instead of purely $[B_3O_9]$ groups in **II**. $[B_3O_8]$ is also a 3-ring unit consisting of two BO_4 and one BO_3. The helical borate chain in **III** is formed by alternative linkage of two $[B_3O_9]$ and one $[B_3O_8]$. Therefore, unlike **II** where all boron atoms are tetrahedrally coordinated, one-sixth of the boron atoms are triangularly coordinated in **III**. The presence of the $[B_3O_8]$ groups in the structure destroys the 3-fold screw axis of the borate chain, leading to lower symmetry for this structure.

The triclinic structure of **III** is a tentative structure model and the atomic parameters are not accurate. However, the basic framework of the structure must be correct not only because of the reasonable fitting to the X-ray powder diffraction pattern but also because of the other characterizations supporting this model. As shown in Figure 1c, the weak absorption peak in the range of $1200-1400$ cm^{-1} in the IR spectrum originates from the vibration of BO_3 groups. The stretching vibration of OH groups at about 3400 cm^{-1} confirms that **III** is a hydrated bismuth borate. In addition, the calculated weight loss (calcd. 1.0 wt %) agrees with the decomposition reaction of $Bi_3[B_6O_{13}(OH)]$ (exp. 2.5 wt %) reasonably well. All these evidences show that the structure of **III** may deviate from the ideal trigonal symmetry as that of **II**. However, by using present tentative structure model, one cannot definitely assign the possible hydrogen position by using BVS.

Helical Borate Chains. The helical borate chains of **II** and **III** are built by sharing two BO_4 groups of 3-ring units; therefore, there are only two types of 3-ring units that can be used to construct helical chains, i.e., $[B_3O_9]$ and $[B_3O_8]$. **II** contains only $[B_3O_9]$ (Figure 6a), and thus the borate chain is $[B_6O_{15}]$ ($[B_6O_{12}F_3]^{9-}$ in BiB_2O_4F). In **III**, the borate chain is composed of alternative stacking of two $[B_3O_9]$ and one $[B_3O_8]$ units (Figure 6b), which results in one-dimensional borate anion of $[B_6O_{14}]$ ($[B_6O_{13}OH]^{9-}$ in $Bi_3[B_6O_{13}(OH)]$). Interestingly, a related infinite helical borate chain was found
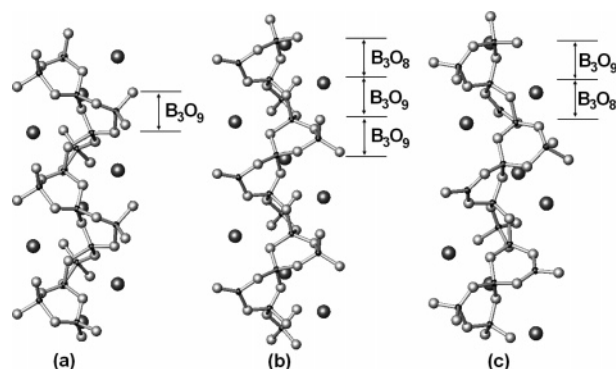
in $Pb_6B_{11}O_{18}(OH)_9$.[29] As shown in Figure 6c, in the helical borate chain of this lead borate, the $[B_3O_9]$ and $[B_3O_8]$ units alternate one after the other, leading to a borate chain with composition of $[B_4O_9]$ (or $[B_6O_{13.5}]$). Therefore, these compounds, **II**, **III**, and $Pb_6B_{11}O_{18}(OH)_9$, could be considered as a helical chain family, which are composed of the two fundamental 3-ring units, $[B_3O_9]$ and $[B_3O_8]$. The compositions of the helical borate chain anions vary according to the $[B_3O_8]:[B_3O_9]$ ratio, which is 0:1 in **II**, 1:2 in **III**, and 1:1 in $Pb_6B_{11}O_{18}(OH)_9$.

Nonlinear Optical Properties. I, II, and **III** crystallize in noncentrosymmetric structures, so they all exhibit second-order nonlinear optical effects (NLO). The measurements were performed on powder samples using KDP as a reference. The normalized intensities of the double-frequency outputs ($\lambda = 532$ nm), which can be used as a measure for the NLO effect, are respectively 0.5, 1.8, and 1.5 for **I, II,** and **III**. Interestingly, $Pb_6B_{11}O_{18}(OH)_9$[29] also shows NLO effect (1.2 times of KDP), which is in the same magnitude as that of **II** and **III**. At present we do not know the structure components that contribute mostly to the NLO effect. However, the same magnitude of the NLO effect found in **II, III,** and $Pb_6B_{11}O_{18}(OH)_9$ may imply that the helical borate chains may play an important role in the nonlinear optical property for these one-dimensional borates.

In conclusion, two hydrated bismuth borates, $Bi[B_4O_6(OH)_2]OH$ (**I**) and $Bi_3[B_6O_{13}(OH)]$ (**III**), and a bismuth fluoroborate, BiB_2O_4F (**II**), were synthesized at low temperatures in a closed system by using boric acid as a flux. All of these bismuth borates (or fluoroborate) contain one-dimensional borate chains. The borate chains in **I** are composed of 3-ring ($2BO_3 + BO_4$) and a BO_3 groups. While in **II** and **III**, the borate chains are helical, which are formed with two fundamental 3-ring units, $[B_3O_9]$ and $[B_3O_8]$. To form a helical borate chain, the 3-ring units need to share two BO_4 groups. Therefore, $[B_3O_9]$ and $[B_3O_8]$ are the only two 3-ring units that can be used to construct the helical borate chains. The cavities on the helical borate chains are occupied by bismuth cations, which are further coordinated by neighboring chains forming 3-dimensional structures. A similar coordination behavior was also reported in the

(29) Yu, Z. T.; Shi, Z.; Jiang, Y. S.; Yuan, H. M.; Chen, J. S. *Chem. Mater.* **2002**, *14*, 1314.

structure of a lead borate, $Pb_6B_{11}O_{18}(OH)_9$. In fact, these three compounds (**II**, **III**, and $Pb_6B_{11}O_{18}(OH)_9$) constitute an interesting family in which the $[B_3O_9]$ and $[B_3O_8]$ units connect alternatively to form the helical borate chains. The NLO properties of these bismuth borates have not yet been fully understood, but the relatively strong effect for those that contain helical borate chains might be an indication that the helical borate chains may play a significant role in the NLO effect.

Supporting Information Available: Table for bond angles of $Bi[B_4O_6(OH)_2]OH$ and BiB_2O_4F; TGA curves of $Bi[B_4O_6(OH)_2]$-OH, BiB_2O_4F, and $Bi_3[B_6O_{13}(OH)]$ (PDF). This material is available free of charge via the Internet at http://pubs.acs.org.

CM050215D